



# Mimetic Discretization of Elliptic PDE with Full Tensor Coefficients

Huy Vu and Jose Castillo

November 2006

Publication Number: CSRCR2006-16

Computational Science &  
Engineering Faculty and Students  
Research Articles

Database Powered by the  
Computational Science Research Center  
Computing Group

## COMPUTATIONAL SCIENCE & ENGINEERING



**SAN DIEGO STATE  
UNIVERSITY**

Computational Science Research Center  
College of Sciences  
5500 Campanile Drive  
San Diego, CA 92182-1245  
(619) 594-3430



# MIMETIC DISCRETIZATION OF ELLIPTIC PDE WITH FULL TENSOR COEFFICIENTS

Huy Vu<sup>a,c</sup>  
Jose Castillo<sup>b,d</sup>

<sup>a</sup> Department of Computer Science, San Diego State University, San Diego, CA 92182, USA.

<sup>b</sup> Department of Mathematics and Statistics, San Diego State University, San Diego, CA 92182, USA.

## ABSTRACT

This work concentrates upon the Mimetic discretization of elliptic partial differential equations (PDE). Numerical solutions are obtained and discussed for one-dimensional ODE on uniform and irregular grids and two-dimensional PDE on uniform grids. The focal point is to develop a scheme that incorporates the full tensor case on uniform grids in 2-D. The numerical results are then compared to previous well-established methods. Based on its conservative properties and global second order of accuracy, this Mimetic scheme shows higher precision in the tests given, especially on the boundaries.

## 1. INTRODUCTION

Mimetic discretization – described as “discretizing a continuum theory” - constructs a discrete mathematical analog with a description of continuum mechanics, in which it preserves the conservation or constitutive law’s properties and behaviors. Mimetic discretizations are represented by discrete operators, such as Divergence and Gradient that satisfy constraints of conservation or constitutive law. These operators are then substituted into the system of partial differential equations or integral equations accordingly. Basically, they mimic the behaviors within the continuum mechanics problems or imitate the symmetry properties of the continuum differential operators to obtain a highly accurate and meaningful interpretation of the underlying physical properties of continuum problems [6] and [7].

Specifically, one example of conservation properties satisfied by differential operators includes the special case of the general Stokes theorem written as

$$\int_M d = \int_{\partial M} , \quad (1.1)$$

in which,  $M$  is a compact oriented  $n$ -manifold with the boundary  $\partial M$ ,  $\omega$  is  $(n-1)$  form on  $M$ , and  $d$  is the exterior derivative of  $\omega$ . Equation (1.1) is applied to the sub-manifolds of  $\mathbb{R}^2$  and  $\mathbb{R}^3$ , hence yields the classical Stokes’ theorem as well as the Divergence theorem and Green’s theorem. The convenient use of Stokes’ Theorem lies at the coordinate free description of continuum mechanics. In addition, Stokes’ Theorem possesses an innate physical interpretation within applications of physics such as electromagnetism and fluid mechanics. These properties of Stokes’ Theorem become essential for building the divergence and gradient operators in the Mimetic Method.

By letting  $\omega = v(t)u(t)$  on the interval  $[0, 1]$ , equation (1.1) becomes the following expression:

---

<sup>c</sup> Email: huykhanhvu@yahoo.com

<sup>d</sup> Email: castillo@myth.sdsu.edu

$$\int_0^1 \frac{dv}{dx} u \, dx + \int_0^1 v \frac{du}{dx} \, dx = v(1)u(1) - v(0)u(0). \quad (1.2)$$

A discrete form of the conservation law needs to be constructed to satisfy local conservation at every cell interval, as well as to fulfill the global conservation for the entire investigated interval. Consequently, these conservation properties will be validated within the underlying region of the boundary value problem.

In figure 1.1, the cell spacing is uniform with a magnitude of  $(h = 1/n)$  over the interval,  $[0, 1]$  in 1-D. Because the investigated interval is divided equally into  $n$  sub-intervals, each node has a coordinate at  $x_i = (i \cdot h)$  in which  $(0 \leq i \leq n)$  including  $x_0$  and  $x_n$  as the left and right boundary nodes, respectively. Each cell has a cell centered point, i.e.,  $[x_i, x_{i+1}]$  includes the center coordinate  $x_{i+1/2}$ .

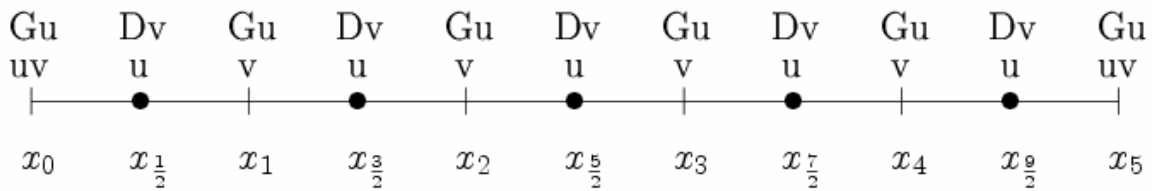


**Figure 1.1. 1-D staggered uniform grid.**

Let  $u(x)$  and  $v(x)$  be two real valued scalar functions and defined on the real-value interval,  $[0, 1]$ . Some investigated function vectors can be descriptively defined as

Vector  $u_c$  as evaluated at the centers of cells:

$$u_c = (u(x_{1/2}), u(x_{3/2}), \dots, u(x_{n-1/2}))^T.$$

Vector  $u_{cb}$  as evaluated at the centers of cells, the left boundary, and the right boundary:

$$u_{cb} = (u(x_0), u(x_{1/2}), u(x_{3/2}), \dots, u(x_{n-1/2}), u(x_n))^T.$$

Vector  $v$  as evaluated at the nodes of cells, including the boundaries:

$$v = (v(x_0), v(x_1), v(x_2), \dots, v(x_n))^T,$$

where  $D$  denotes the difference approximation for the divergence operator as applied upon the function at the nodes of cells, and  $G$  denotes the difference approximation for the gradient operator as applied upon the function at the cell centers and boundaries.

## 2. DISCRETE DIVERGENCE THEOREM IN CASTILLO-GRONE APPROACH

In general, the Castillo-Grone approach [4], as expressed by the law of conservation for equation (1.2), is depicted in a discrete inner product form over the staggered grids by the following:

$$\langle \hat{D}v, u_c \rangle_Q + \langle v, Gu_{cb} \rangle_P = \langle Bv, u_{cb} \rangle, \quad (2.1)$$

in which the weights  $P$  and  $Q$  are positive definite matrices that are used to determine the forms of the  $D$  and  $G$  matrices, respectively.  $\hat{D}$  is the matrix  $D$  augmented with the top and bottom rows containing only zeros.

Let  $Q$  be the identity matrix in  $\mathbb{R}^{(n+2) \times (n+2)}$  and  $P$  be within  $\mathbb{R}^{(n+1) \times (n+1)}$  equal to

$$P = \begin{bmatrix} 1/2 & 0 & \cdots & \cdots & 0 \\ 0 & 1 & & & \vdots \\ \vdots & & \ddots & & \vdots \\ \vdots & & & 1 & 0 \\ 0 & \cdots & \cdots & 0 & 1/2 \end{bmatrix}, \quad (2.2)$$

then the support operator method can be obtained [8]. In this method, divergence is second order over the interior of the domain as well as the boundaries ( $D_{2-2-2}$ ) and its gradient is second order within the interior of the domain but first order at the boundaries ( $G_{1-2-1}$ ).

The boundary operator  $B$  for support operator, called  $B_1$ , is defined in the subspace  $\mathbb{R}^{(n+2) \times (n+1)}$  as

$$B_1 = \begin{bmatrix} -1 & 0 & \cdots & \cdots & 0 \\ 0 & 0 & & & \vdots \\ \vdots & & \ddots & & \vdots \\ \vdots & & & 0 & 0 \\ 0 & \cdots & \cdots & 0 & 1 \end{bmatrix} \in \mathbb{R}^{(n+2) \times (n+1)}. \quad (2.3)$$

These matrices in combination with the law of conservation, equation (2.1), will yield matrix operators  $D$  and  $G$  for the Support Operators Method in 1-D staggered grids [8], such that:

$$hD = \begin{bmatrix} -1 & 1 & 0 & \cdots & 0 \\ 0 & \ddots & \ddots & & \\ \vdots & & \ddots & \ddots & \\ 0 & \cdots & 0 & -1 & 1 \end{bmatrix} \in \mathbb{R}^{n \times (n+1)} \quad (2.4)$$

and

$$hG = \begin{bmatrix} -2 & 2 & 0 & \cdots & \cdots & 0 \\ 0 & -1 & 1 & & & \vdots \\ \vdots & & \ddots & \ddots & & \vdots \\ \vdots & & & -1 & 1 & 0 \\ 0 & \cdots & \cdots & 0 & -2 & 2 \end{bmatrix} \in \mathbb{R}^{(n+1) \times (n+2)}. \quad (2.5)$$

### 3. MIMETIC OPERATORS

The Mimetic method discussed in [4] can be used to construct discrete divergence and gradient operators of any even order of accuracy. Here the second order operators will be the main focus for study and analysis. The Mimetic operators are constructed with the Castillo-Grone method are second order within the interior as well as at the boundaries. Consequently, these operators are alternatively called as 2-2-2 scheme operators.

The boundary operator  $B$  for the second order Mimetic discretization study, denoted as  $\tilde{B}$ , is

$$\tilde{\mathbf{B}} = \begin{bmatrix} -1 & 0 & 0 & \dots & \dots & 0 & 0 & 0 \\ \frac{1}{8} & -\frac{1}{8} & 0 & \dots & \dots & 0 & 0 & 0 \\ -\frac{1}{8} & \frac{1}{8} & 0 & \dots & \dots & 0 & 0 & 0 \\ 0 & 0 & 0 & \ddots & & 0 & 0 & 0 \\ \vdots & \vdots & \vdots & \ddots & \ddots & \vdots & \vdots & \vdots \\ 0 & 0 & 0 & \dots & \dots & 0 & 0 & 0 \\ 0 & 0 & 0 & \dots & \dots & 0 & -\frac{1}{8} & \frac{1}{8} \\ 0 & 0 & 0 & \dots & \dots & 0 & \frac{1}{8} & -\frac{1}{8} \\ 0 & 0 & 0 & \dots & \dots & 0 & 0 & 1 \end{bmatrix} \in \mathbb{R}^{(n+2) \times (n+1)}. \quad (3.1)$$

The use of both  $\mathbf{B}_1$  and  $\tilde{\mathbf{B}}$  boundary operators is investigated for the Castillo-Grone Mimetic discretization. Moreover,  $\mathbf{D}$  and  $\mathbf{Q}$  satisfy a discrete analogue of the divergence theorem, as in equation (2.1):

$$\langle \mathbf{D}\mathbf{v}, \mathbf{u}_c \rangle_{\mathbf{Q}} + \langle \mathbf{v}, \mathbf{G}\mathbf{u}_{cb} \rangle_{\mathbf{P}} = \langle \tilde{\mathbf{B}}\mathbf{v}, \mathbf{u}_{cb} \rangle,$$

where  $\mathbf{Q}$  is the identity and  $\mathbf{P}$  is,

$$\mathbf{P} = \begin{bmatrix} \frac{3}{8} & 0 & \dots & \dots & \dots & \dots & 0 \\ 0 & \frac{9}{8} & \ddots & & & & \vdots \\ \vdots & \ddots & 1 & \ddots & & & \vdots \\ \vdots & & \ddots & \ddots & \ddots & & \vdots \\ \vdots & & & \ddots & 1 & \ddots & \vdots \\ \vdots & & & & \ddots & \frac{9}{8} & 0 \\ 0 & \dots & \dots & \dots & \dots & 0 & \frac{3}{8} \end{bmatrix}. \quad (3.2)$$

Therefore, the Mimetic second order divergence operator  $\mathbf{D}$  and the gradient  $\mathbf{G}$  on 1-D uniform grids can be inclusively determined from the law of conservation [4]. Both Mimetic divergence and gradient are second order within the interior of the domain as well as at the boundaries ( $\mathbf{D}_{2-2-2}$  and  $\mathbf{G}_{2-2-2}$  respectively):

$$\mathbf{hD} = \begin{bmatrix} -1 & 1 & 0 & \dots & 0 \\ 0 & \ddots & \ddots & \ddots & \ddots \\ \vdots & & \ddots & \ddots & \ddots \\ 0 & \dots & 0 & -1 & 1 \end{bmatrix} \in \mathbb{R}^{n \times (n+1)} \quad (3.3)$$

$$\mathbf{hG} = \begin{bmatrix} -\frac{8}{3} & 3 & -\frac{1}{3} & \dots & \dots & 0 \\ 0 & -1 & 1 & & & \vdots \\ \vdots & & \ddots & \ddots & & \vdots \\ \vdots & & & -1 & 1 & 0 \\ 0 & \dots & \dots & \frac{1}{3} & -3 & \frac{8}{3} \end{bmatrix} \in \mathbb{R}^{(n+1) \times (n+2)} \quad (3.4)$$

In figure 3.1, the non-uniform grid constitutes the difference in spacing of divided sub-intervals or cells. Consequently, their discrete Gradient and Divergence equations are different from those in the case of uniform grids. Both discrete Gradient and Divergence operators were discussed in [10].

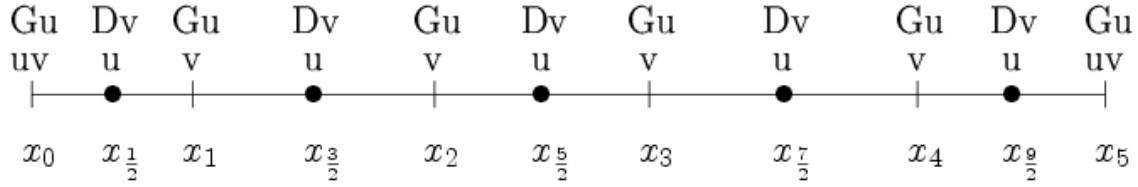


**Figure 3.1. 1-D staggered non-uniform grid.**

Basically, the Gradient Operators for the non-uniform staggered grids over the investigated interval that is composed of  $n$  non-uniform divided sub-intervals have the following expressions:

i. The gradient as defined on the left boundary node is:

$$(\text{Gu})_0 = \frac{-8u(x_0) + 9u(x_{1/2}) - u(x_{3/2})}{-8(x_0) + 9(x_{1/2}) - (x_{3/2})}, \quad (3.5a)$$

where  $x_0$  is the left boundary nodal point,  $x_{1/2}$  is the center of the first divided sub-interval, and  $x_{3/2}$  is the center of the second divided sub-interval.

ii. The gradient as defined at an interior nodal point, excluding the boundary nodes is:

$$(\text{Gu})_i = \frac{u(x_{i+1/2}) - u(x_{i-1/2})}{(x_{i+1/2}) - (x_{i-1/2})}, \quad (3.6a)$$

where  $i = 1, 2, \dots, n-1$ ;  $x_{i+1/2}$  and  $x_{i-1/2}$  are centers of two adjacent divided sub-intervals,  $[x_i, x_{i+1}]$  and  $[x_{i-1}, x_i]$ , respectively.

iii. The gradient as defined on the right boundary node is:

$$(\text{Gu})_n = \frac{-8u(x_n) + 9u(x_{n-1/2}) - u(x_{n-3/2})}{-8(x_n) + 9(x_{n-1/2}) - (x_{n-3/2})}, \quad (3.7a)$$

where  $x_{n-1/2}$  and  $x_{n-3/2}$  are the centers of the last two divided sub-intervals,  $[x_{n-1}, x_n]$  and  $[x_{n-2}, x_{n-1}]$ , respectively.

Let the spacing of the divided sub-interval of  $[x_{i-1}, x_i]$ ,  $h_i$ , be

$$h_i = x_i - x_{i-1}. \quad (3.8)$$

Since  $x_{i-1/2}$  is the center of the divided sub-interval  $[x_{i-1}, x_i]$ ,

$$x_{i-1/2} = \frac{x_{i-1} + x_i}{2}, \quad (3.9)$$

in which  $i = 1, 2, \dots, n$ . Thus equations (3.5a), (3.6a), and (3.7a) can be expressed in terms of the solution function  $u$  and cell spacing  $h_i$ :

$$(\text{Gu})_0 = \frac{-16u(x_0) + 18u(x_{1/2}) - 2u(x_{3/2})}{7h_1 - h_2}, \quad (3.5b)$$

$$(\text{Gu})_i = \frac{2[u(x_{i+1/2}) - u(x_{i-1/2})]}{h_i + h_{i+1}}, \quad (3.6b)$$

$$(\text{Gu})_n = \frac{2u(x_{n-3/2}) - 18u(x_{n-1/2}) + 16u(x_n)}{7h_n - h_{n-1}} \quad (3.7b)$$

respectively, where  $i = 1, 2, \dots, n-1$  for equation (3.6b).

The Divergence on Non-Uniform Grids was also discussed in [10]. The Divergence Operator is evaluated at the center of each divided sub-interval where

$$(\mathbf{Dv})_{i+\frac{1}{2}} = \frac{v(x_{i+1}) - v(x_i)}{x_{i+1} - x_i}. \quad (3.10a)$$

This leads to

$$(\mathbf{Dv})_{i+\frac{1}{2}} = \frac{v(x_{i+1}) - v(x_i)}{h_{i+1}}, \quad (3.10b)$$

in which,  $i = 0, 1, \dots, n-1$  and  $v$  is the function evaluated at the nodes, including the boundaries.

#### 4. THE 2-2-2 SCHEME MIMETIC DISCRETIZATION ON 1-D GRIDS

The boundary value problem is depicted with an Ordinary Differential Equation (ODE) by the following:

$$-\operatorname{div}(\operatorname{grad}(u)) = f(x) \text{ on } [0,1]. \quad (4.1)$$

The Robin boundary conditions are applied on the left and the right boundaries of the interval as

$$u(0) - u'(0) = lb, \quad (4.2)$$

$$u(1) + u'(1) = rb. \quad (4.3)$$

In the case of using the discrete operators on this ODE (4.1) including the boundary equations (4.2) and (4.3),  $\mathbf{D}$  and  $\mathbf{G}$ , which are the Divergence and Gradient Operators respectively, will be replacing the corresponding continuous operators. Thus, the discretization of this boundary value problem becomes

$$(\mathbf{A} + \mathbf{BG} - \mathbf{L})\mathbf{u} = \mathbf{b}, \quad (4.4)$$

where matrix  $\mathbf{A}$  within  $\mathbf{R}^{(n+2) \times (n+2)}$  is defined as

$$\mathbf{A} = \begin{bmatrix} 1 & 0 & \cdots & \cdots & 0 \\ 0 & 0 & \ddots & & \vdots \\ \vdots & \ddots & \ddots & \ddots & \vdots \\ \vdots & & \ddots & 0 & 0 \\ 0 & \cdots & \cdots & 0 & 1 \end{bmatrix} \in \mathbf{R}^{(n+2) \times (n+2)}. \quad (4.5)$$

The discrete Laplacian Operator,  $\mathbf{L}$ , within  $\mathbf{R}^{(n+2) \times (n+2)}$  can be expressed as

$$\mathbf{L} = \begin{bmatrix} 0 & \cdots & 0 \\ & \mathbf{DG} & \\ 0 & \cdots & 0 \end{bmatrix} \in \mathbf{R}^{(n+2) \times (n+2)} \quad (4.6)$$

The right hand side vector,  $\mathbf{b}$ , within  $\mathbf{R}^{n+2}$  is determined as

$$\mathbf{b} = (lb, f(x_{\frac{1}{2}}), f(x_{\frac{3}{2}}), \dots, f(x_{n-\frac{1}{2}}), rb)^T, \quad (4.7)$$

where  $lb$  and  $rb$  are the right-hand side scalar values for the left and right boundary conditions, respectively. Right hand side function,  $f$ , is evaluated at the central points of each divided sub-interval. Constants and drive the Dirichlet and Neumann terms in the boundary conditions, respectively.

The solution vector  $\mathbf{u}$ , within  $\mathbf{R}^{n+2}$  is defined as

$$\mathbf{u} = (u(x_0), u(x_{1/2}), u(x_{3/2}), \dots, u(x_{n-1/2}), u(x_n))^T. \quad (4.8a)$$

If the  $\tilde{\mathbf{B}}$  Operator is used instead of the  $\mathbf{B}_1$  Operator, then the discretization of the boundary value problem becomes

$$(\mathbf{A} + \tilde{\mathbf{B}}\mathbf{G} - \mathbf{L})\tilde{\mathbf{u}} = \mathbf{b}, \quad (4.9)$$

where  $\tilde{\mathbf{u}}$  is the solution vector within  $\mathbf{R}^{n+2}$  corresponding to  $\tilde{\mathbf{B}}$  Operator in equation (4.9),

$$\tilde{\mathbf{u}} = (\tilde{u}(x_0), \tilde{u}(x_{1/2}), \tilde{u}(x_{3/2}), \dots, \tilde{u}(x_{n-1/2}), \tilde{u}(x_n))^T. \quad (4.8b)$$

## 5. THE MIMETIC DISCRETIZATION ON 2-D UNIFORM GRIDS

The main goal is to investigate the use of Mimetic Discretization for solving the elliptic partial differential equation (PDE) with the mathematical model in 2-D such that:

$$-\nabla \cdot (\mathbf{K} \cdot \nabla u(x, y)) = f(x, y) \text{ on } (x, y) \in V, \quad (5.1)$$

which can be also written as,

$$-\text{div}(\mathbf{K} \cdot \text{grad } u) = f \text{ on } V \quad (5.2)$$

where  $V$  is  $[(x_L, x_U) \times (y_L, y_U)]$ .

The solution to this elliptic equation,  $u(x, y)$  involves the pressure of the flow in the reservoir simulation problem, where  $\mathbf{K}$  is a symmetric, positive definite and second order tensor matrix. Scalars  $x_L$  and  $x_U$  are the lower and upper boundaries, respectively, in the  $x$ -direction, and  $y_L$  and  $y_U$  are the lower and upper boundaries, respectively, in the  $y$ -direction within 2-D space. Let  $V$  be the two-dimensional space region, except at the boundaries.

Uniform grids are defined by the spatial steps,  $\Delta x$  and  $\Delta y$ , inscribed within  $[x_L, x_U]$  and  $[y_L, y_U]$  respectively.

In the case of Robin Boundary Conditions, at the boundary  $\partial V$ :

$$u + \mathbf{K} \cdot \text{grad } u = \phi \text{ on } (x, y) \in \partial V, \quad (5.3)$$

where  $\phi$  is the scalar value in the Dirichlet term,  $\psi$  is the scalar value in the Neumann term, and  $f$  is the given right-hand function at the boundary,  $\partial V$ . In the case of ( $\psi = 0$ ), equation (7.3) reduces to Dirichlet boundary conditions on  $\partial V$ . Physically, the flux,  $w$ , in this particular context is defined as

$$w = \mathbf{G} u = \mathbf{K} \cdot \text{grad } u, \quad (5.4)$$

where  $\mathbf{G}$  notation for 2-D case has been changed from the 1-D case, in which  $\mathbf{G}$  is denoted as Gradient. In 2-D,  $\mathbf{G}$  is applied on the function  $u$  becoming the flux. To write the elliptic PDE problem in a matrix equation representation, let  $\mathbf{A}$ ,  $\mathbf{D}$ , and  $\mathbf{B}$  be matrix operators as defined in [9]:

$$\mathbf{A}u = \begin{cases} -\text{div}(\mathbf{K} \cdot \text{grad } u) & \text{with } (x, y) \in V \\ u + \mathbf{K} \cdot \text{grad } u & \text{with } (x, y) \in \partial V, \end{cases} \quad (5.5)$$

$$\mathbf{D}w = \begin{cases} -\text{div}(\mathbf{G}u) & \text{with } (x, y) \in V \\ 0 & \text{with } (x, y) \in \partial V, \end{cases} \quad (5.6)$$

where  $\mathbf{D}$  is the Divergence Operator on the flux.

$$\mathbf{B}u = \begin{cases} 0 & \text{with } (x, y) \in V \\ u + \mathbf{G} u & \text{with } (x, y) \in \partial V, \end{cases} \quad (5.7)$$

where  $\mathbf{B}$  is the Boundary Operator, and the Robin boundary conditions are used.

Also let  $F$  be a vector defined as:

$$F = \begin{cases} f & \text{with } (x, y) \in V \\ & \text{with } (x, y) \in \partial V \end{cases} \quad (5.8)$$

where  $F$  is the right-hand side vector function of the matrix equation system.

Therefore, the left hand side matrix, Operator  $A$  is represented by the following expression:

$$A = B + D \cdot G. \quad (5.9)$$

Moreover, the elliptic partial differential equation including the boundary conditions can be expressed in terms of the matrix equation system as:

$$Bu + D \cdot Gu = F. \quad (5.10)$$

The accuracy for solving this elliptic partial differential equation depends precisely upon the discrete Divergence operator  $D$ , discrete operator  $G$  for the flux, and discrete Boundary Operator  $B$ . Both discrete  $D$  and  $G$  Operators will be incorporated with the  $B_1$  Boundary Operator to determine the matrix equation system for 2-D case.

For a better understanding of 2-D discretization, two figures are displayed in order to interpret the layout of the Gradient, Divergence, solution function, and the tensor coefficients. Figure 5.1 is an illustration of (5x5) 2-D staggered uniform grids with a natural lexicographic ordering for Divergence, Gradient, and Tensor components whereas figure 5.2 is an illustration of (5x5) 2-D staggered uniform grids for the coordination of various solution function points.

## 5.1. Definition of 2-D Uniform Grids

Let the investigated region be either a rectangle or a square in 2-D space, where  $i$  is denoted by the subscript in the  $x$ -direction,  $j$  is denoted by the subscript in the  $y$ -direction, and the interval on the  $x$ -direction is divided into  $n$  equal sub-intervals, while the interval in the  $y$ -direction is divided into  $m$  equal sub-intervals. The domain can be discretized as follows:

In the  $x$ -direction:  $x_i = i \cdot \Delta x$

The subscript  $i$  is constrained by:

$$0 \leq i \leq n. \quad (5.11)$$

Hence, the investigated interval is defined on the interval  $[x_0, x_n]$ .

The grid size on the divided sub-interval is defined by:

$$\Delta x_{i+1} = x_{i+1} - x_i, \quad (5.12)$$

with  $i = 0, 1, \dots, n-1$ . Hence, there are  $(n+1)$  nodes and  $n$  sub-intervals.

All sub-intervals are equally divided, hence:

$$\Delta x_1 = \Delta x_2 = \dots = \Delta x_n = \left( \frac{x_n - x_0}{n} \right). \quad (5.13)$$

The center of each divided sub-interval has the following coordinate:

$$x_{i+1/2} = \left( \frac{x_i + x_{i+1}}{2} \right). \quad (5.14)$$

Similarly, in the  $y$ -direction,  $y_j = j \cdot \Delta y$  where subscript  $j$  is constrained by:

$$0 \leq j \leq m. \quad (5.15)$$

The grid size of each sub-interval is defined by:

$$\Delta y_{i+1} = y_{i+1} - y_i. \quad (5.16)$$

with  $j = 0, 1, \dots, m-1$ ; there are  $(m+1)$  nodes and  $m$  sub-intervals.

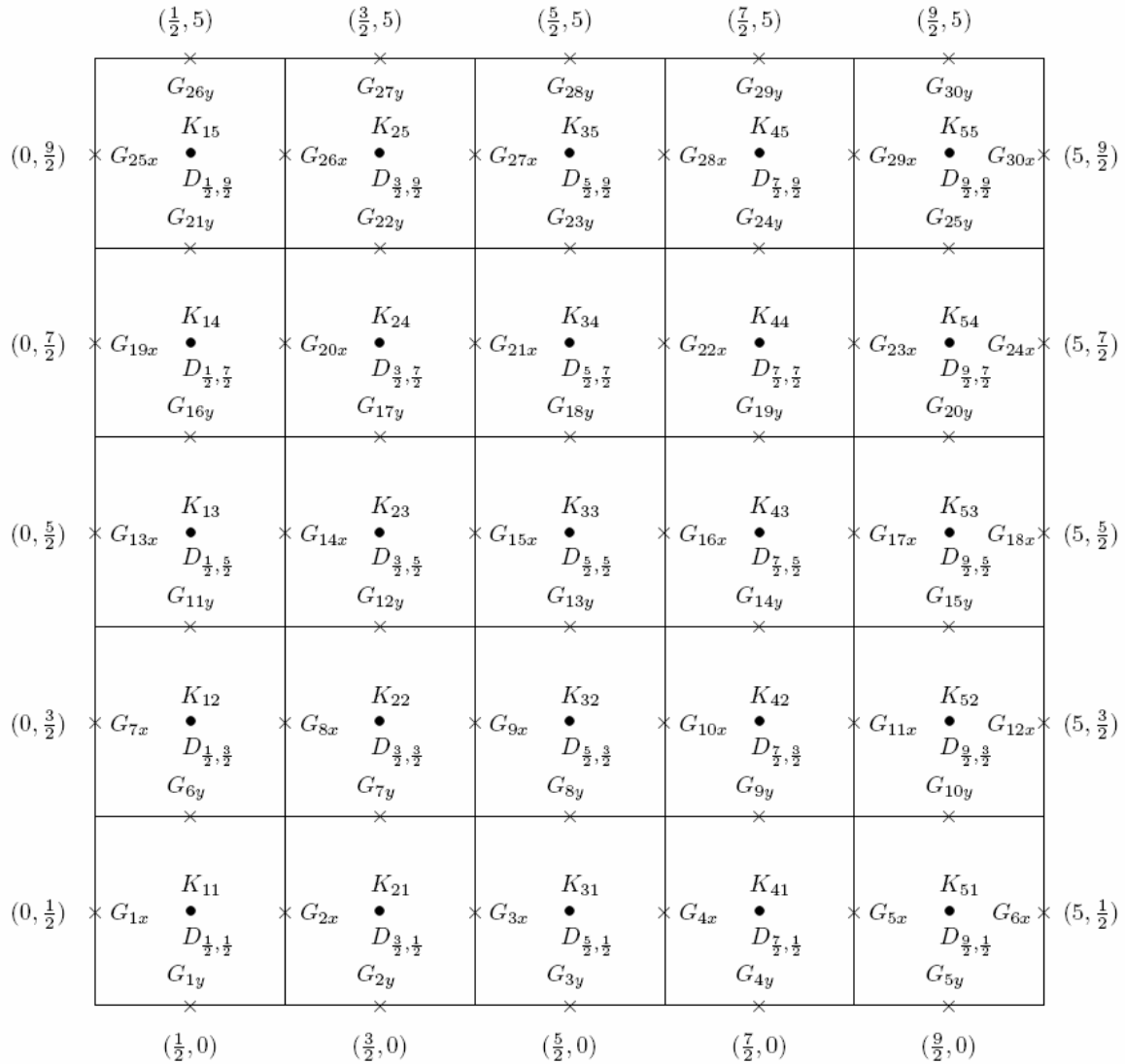


**Figure 5.1. Gradient, divergence, and tensor components on 2-D uniform grids.**

All sub-intervals are equally divided, i.e,

$$y_1 = y_2 = \dots = y_m = \left( \frac{y_m - y_0}{m} \right). \quad (5.17)$$

In 2-D, the grid cells are divided equally and inscribed within four nodes,  $(x_i, y_i)$ ,  $(x_{i+1}, y_i)$ ,  $(x_i, y_{i+1})$ ,  $(x_{i+1}, y_{i+1})$ . The area of the cell is denoted as  $VC_{i+1,j+1}$ . All grid cells are either rectangles or squares dependent upon the sizes of x-coordinate and y-coordinate sub-divided intervals. Hence,

$$VC_{i+1,j+1} = x_{i+1} \cdot y_{i+1}. \quad (5.18)$$

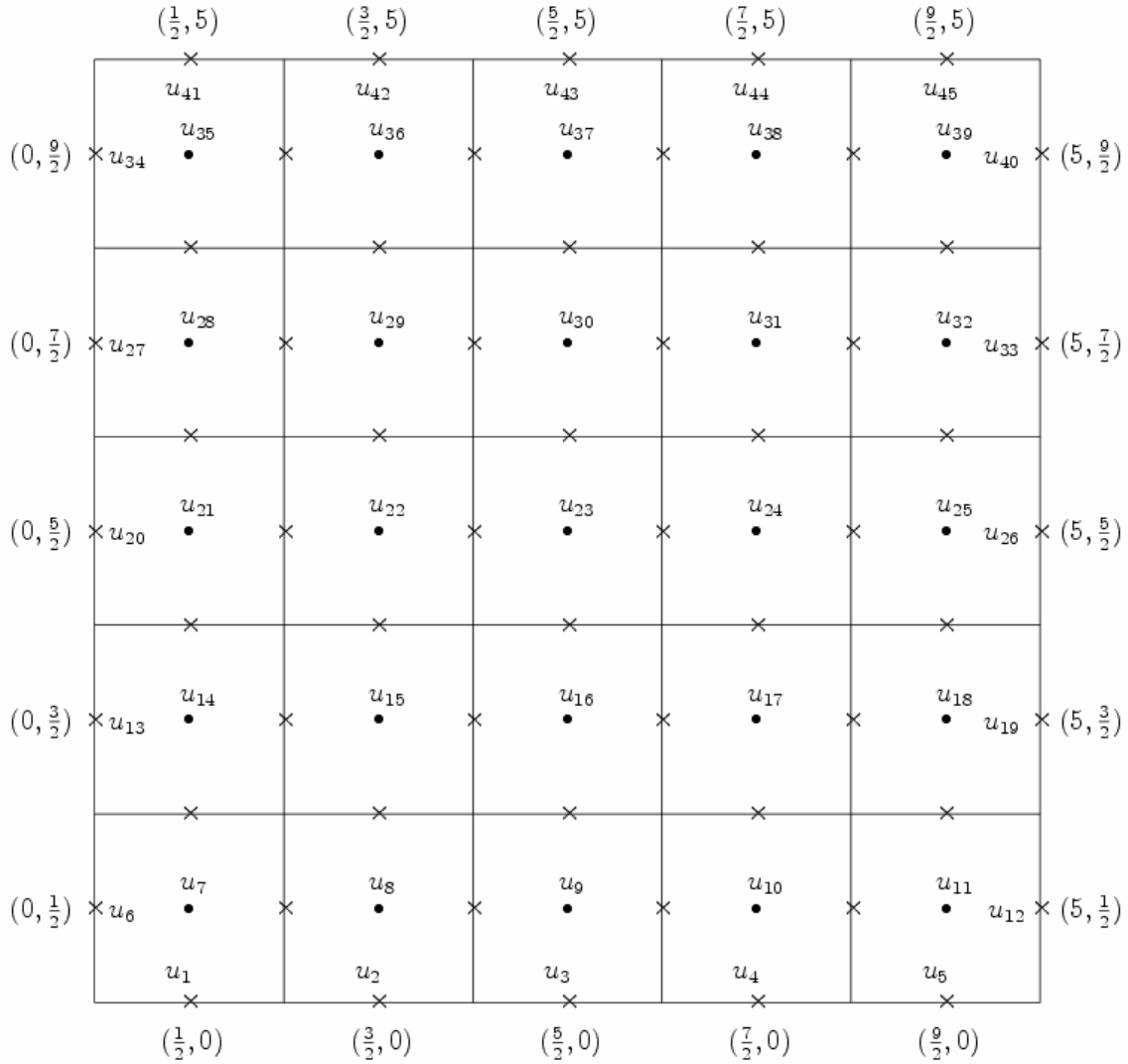


**Figure 5.2. Solution function on 2-D staggered uniform grids.**

In the particular case of uniform grids, all of the cell volumes are equal:

$$\begin{aligned}
 & VC_{1,1} = VC_{1,2} = \dots = VC_{1,m} \\
 & = VC_{2,1} = VC_{2,2} = \dots = VC_{2,m} \\
 & \dots \\
 & = VC_{n,1} = VC_{n,2} = \dots = VC_{n,m} .
 \end{aligned} \tag{5.19}$$

## 5.2. Definition of Discrete Tensor Coefficient

In the general case, if  $K$  is a full tensor expressed by the following (2x2) Matrix:

$$K = \begin{bmatrix} K_{11} & K_{12} \\ K_{21} & K_{22} \end{bmatrix}, \tag{5.20}$$

in which  $K_{11}$  is referred to  $K_x$ ,  $K_{22}$  is referred to  $K_y$ ,  $K_{12}$  is referred to  $K_{xy}$ , and  $K_{21}$  is referred to as  $K_{yx}$ . Moreover, for some cases, Tensor  $K$  is just a diagonal tensor taking the form:

$$\mathbf{K} = \begin{bmatrix} \mathbf{K}_{11} & 0 \\ 0 & \mathbf{K}_{22} \end{bmatrix}. \quad (5.21)$$

Occasionally, the diagonal tensor  $\mathbf{K}$  takes the simple form as an identity matrix with  $\mathbf{K}_{11} = \mathbf{K}_{22} = 1$ , i.e.,

$$\mathbf{K} = \begin{bmatrix} 1 & 0 \\ 0 & 1 \end{bmatrix}. \quad (5.22)$$

Components of Tensor,  $\mathbf{K}$  can be defined using continuous or discontinuous functions which could cause problems for numerical method implementation.

As described in figure 7.1 of the staggered 2-D uniform grids, the tensor coefficient  $\mathbf{K}$  is defined at the centers of grid cells, and is denoted as:

$$\mathbf{K}(x_{i+1/2}, y_{j+1/2}) = \mathbf{K}_{i+1/2, j+1/2},$$

where  $i = 0, 1, \dots, n-1$  and  $j = 0, 1, \dots, m-1$ .

### 5.3. Definition of Discrete Solution Function

Figure 5.2 describes the staggered distribution of the solution function along the grids. At the interior, the solution function  $u$  is defined at the centers of grid cells and is denoted as:

$$u(x_{i+1/2}, y_{j+1/2}) = u_{i+1/2, j+1/2},$$

for  $i = 0, 1, \dots, n-1$  and  $j = 0, 1, \dots, m-1$ .

At the boundaries, the solution function  $u$  is defined at the center of the boundary edges including the left, right, bottom, and top edges. On the vertical edges, the solution function is denoted as,

i. For the left boundary ( $x = x_0$ ):

$$u(x_0, y_{j+1/2}) = u_{0, j+1/2}.$$

ii. For the right boundary ( $x = x_n$ ):

$$u(x_n, y_{j+1/2}) = u_{n, j+1/2}.$$

On the horizontal edges, the solution function is denoted as follows:

i. For the bottom boundary ( $y = y_0$ ):

$$u(x_{i+1/2}, y_0) = u_{i+1/2, 0}.$$

ii. For the top boundary ( $y = y_m$ ):

$$u(x_{i+1/2}, y_m) = u_{i+1/2, m},$$

where  $i = 0, 1, \dots, n-1$  and  $j = 0, 1, \dots, m-1$ .

### 5.4. Definition of Boundary Operator

Similarly to the case above, the Boundary Operator  $B$  is defined at the center of edges of the boundary grid cells:

On the vertical edges,  $B$  is denoted as follows:

i. For the left boundary:

$$B(x_0, y_{j+1/2}) = B_{0, j+1/2}.$$

ii. For the right boundary,

$$B(x_n, y_{j+1/2}) = B_{n, j+1/2}.$$

On the horizontal edges,  $B$  is denoted as follows:

i. For the bottom boundary,

$$B(x_{i+1/2}, y_0) = B_{i+1/2, 0}.$$

ii. For the top boundary,

$$B(x_{i+1/2}, y_m) = B_{i+1/2, m},$$

where  $i = 0, 1, \dots, n-1$  and  $j = 0, 1, \dots, m-1$ . The boundary operator is applied upon the gradient operator  $G$  to create the (BG) Operator in the boundary condition equations.

## 5.5. Definition of Discrete G Operator

The discrete  $G$  operator is defined separately in each component; the  $x$ -component denoted as  $G_x$  and the  $y$ -component denoted as  $G_y$ . The natural ordering is shown in figure 5.1 for both the  $x$ - and  $y$ -components. For  $G_x$ , it is evaluated at the centers of vertical edges and is denoted as:

$$G_{k_x} u = Gu(x_i, y_{j+1/2}) = G_{i, j+1/2},$$

where  $i = 0, 1, \dots, n, j = 0, 1, \dots, m-1$ , and  $k$  is an integer assigned by natural ordering. Hence,  $k$  is defined as

$$k = j(n+1) + (i+1);$$

then  $k$  is iterated numerically as:

$$k = 1, 2, \dots, (m)(n+1).$$

For  $G_y$ , the gradient is evaluated at the centers of horizontal edges and will be denoted as:

$$G_{t_y} u = Gu(x_{i+1/2}, y_j) = G_{i+1/2, j},$$

where  $i = 0, 1, \dots, n-1, j = 0, 1, \dots, m$ , and  $t$  is an integer assigned by natural numeric ordering. Hence,  $t$  is defined as

$$t = i(m+1) + (j+1),$$

then  $t$  is iterated numerically as:

$$t = 1, 2, \dots, n(m+1).$$

## 5.6. Definition of Discrete D Operator

At the interior, the discrete Divergence Operator is defined on the function  $v$  at the centers of the grid cells as:

$$Dv(x_{i+1/2}, y_{j+1/2}) = Dv_{i+1/2, j+1/2}.$$

## 5.7. Definition of Adjusted Mimetic Gradient

Let  $\tilde{G}$  be the adjusted gradient operator in either  $x$ - or  $y$ -component and approximated as,

$$\tilde{G} \cong \text{grad}.$$

As  $G$  be the gradient for  $x$ - and  $y$ -component. Thus the relation of  $\tilde{G}$  and  $G$  is defined as

$$G = K \cdot \tilde{G}.$$

### 5.7.1. Adjusted Gradient on the X-Component

At the left boundary:

$$(\tilde{G}u)_{(0, j+1/2)} = \left(\frac{1}{x}\right) \left[ \left(-\frac{8}{3}\right)u_{0, j+1/2} + (3)u_{1/2, j+1/2} - \left(\frac{1}{3}\right)u_{3/2, j+1/2} \right], \quad (5.23)$$

where  $j = 0, 1, 2, \dots, m-1$  and  $x$  is the divided sub-interval of the  $x$ -component.

On the interior:

$$(\tilde{\mathbf{G}}\mathbf{u})_{(i,j+\frac{1}{2})} = \left(\frac{1}{x}\right)[\mathbf{u}_{i+\frac{1}{2},j+\frac{1}{2}} - \mathbf{u}_{i-\frac{1}{2},j+\frac{1}{2}}], \quad (5.24)$$

where  $i = 1, 2, \dots, n$  and  $j = 0, 1, \dots, m-1$ .

At the right boundary:

$$(\tilde{\mathbf{G}}\mathbf{u})_{(n,j+\frac{1}{2})} = \left(\frac{1}{x}\right)\left[\left(\frac{1}{3}\right)\mathbf{u}_{n-\frac{3}{2},j+\frac{1}{2}} - (3)\mathbf{u}_{n-\frac{1}{2},j+\frac{1}{2}} + \left(\frac{8}{3}\right)\mathbf{u}_{n,j+\frac{1}{2}}\right], \quad (5.25)$$

where  $j = 0, 1, \dots, m-1$ .

### 5.7.2. Adjusted Gradient on the Y-Component

At the bottom boundary:

$$(\tilde{\mathbf{G}}\mathbf{u})_{(i+\frac{1}{2},0)} = \left(\frac{1}{y}\right)\left[-\left(\frac{8}{3}\right)\mathbf{u}_{i+\frac{1}{2},0} + (3)\mathbf{u}_{i+\frac{1}{2},\frac{1}{2}} - \left(\frac{1}{3}\right)\mathbf{u}_{i+\frac{1}{2},\frac{3}{2}}\right], \quad (5.26)$$

where  $i = 0, 1, \dots, n-1$  and  $y$  is the divided sub-interval of the y-component.

On the interior:

$$(\tilde{\mathbf{G}}\mathbf{u})_{(i+\frac{1}{2},j)} = \left(\frac{1}{y}\right)[\mathbf{u}_{i+\frac{1}{2},j+\frac{1}{2}} - \mathbf{u}_{i+\frac{1}{2},j-\frac{1}{2}}], \quad (5.27)$$

where  $j = 1, 2, \dots, m$  and  $i = 0, 1, \dots, n-1$ .

At the top boundary:

$$(\tilde{\mathbf{G}}\mathbf{u})_{(i+\frac{1}{2},m)} = \left(\frac{1}{y}\right)\left[\left(\frac{1}{3}\right)\mathbf{u}_{i+\frac{1}{2},m-\frac{3}{2}} - (3)\mathbf{u}_{i+\frac{1}{2},m-\frac{1}{2}} + \left(\frac{8}{3}\right)\mathbf{u}_{i+\frac{1}{2},m}\right], \quad (5.28)$$

where  $i = 0, 1, \dots, n-1$ .

### 5.7.3. Gradient on the X-Component

The discrete gradient on x- component in 2-D is determined with the scheme as described in [1], [2], and [3].

At the left boundary,

$$\begin{aligned} (\mathbf{G}\mathbf{u})_{(0,j+\frac{1}{2})} &= (\mathbf{K}_{11})_{(0,j+\frac{1}{2})} (\tilde{\mathbf{G}}\mathbf{u})_{(0,j+\frac{1}{2})} \\ &+ \left(\frac{1}{2}\right)[(\mathbf{K}_{12})_{(\frac{1}{2},j)} (\tilde{\mathbf{G}}\mathbf{u})_{(\frac{1}{2},j)} + (\mathbf{K}_{12})_{(\frac{1}{2},j+1)} (\tilde{\mathbf{G}}\mathbf{u})_{(\frac{1}{2},j+1)}]. \end{aligned} \quad (5.29)$$

On the interior,

$$\begin{aligned} (\mathbf{G}\mathbf{u})_{(i,j+\frac{1}{2})} &= (\mathbf{K}_{11})_{(i,j+\frac{1}{2})} (\tilde{\mathbf{G}}\mathbf{u})_{(i,j+\frac{1}{2})} \\ &+ \left(\frac{1}{4}\right)[(\mathbf{K}_{12})_{(i-\frac{1}{2},j)} (\tilde{\mathbf{G}}\mathbf{u})_{(i-\frac{1}{2},j)} + (\mathbf{K}_{12})_{(i+\frac{1}{2},j)} (\tilde{\mathbf{G}}\mathbf{u})_{(i+\frac{1}{2},j)} \\ &+ (\mathbf{K}_{12})_{(i-\frac{1}{2},j+1)} (\tilde{\mathbf{G}}\mathbf{u})_{(i-\frac{1}{2},j+1)} + (\mathbf{K}_{12})_{(i+\frac{1}{2},j+1)} (\tilde{\mathbf{G}}\mathbf{u})_{(i+\frac{1}{2},j+1)}]. \end{aligned} \quad (5.30)$$

At the right boundary,

$$\begin{aligned} (\mathbf{G}\mathbf{u})_{(n,j+\frac{1}{2})} &= (\mathbf{K}_{11})_{(n,j+\frac{1}{2})} (\tilde{\mathbf{G}}\mathbf{u})_{(n,j+\frac{1}{2})} \\ &+ \left(\frac{1}{2}\right)[(\mathbf{K}_{12})_{(n-\frac{1}{2},j)} (\tilde{\mathbf{G}}\mathbf{u})_{(n-\frac{1}{2},j)} + (\mathbf{K}_{12})_{(n-\frac{1}{2},j+1)} (\tilde{\mathbf{G}}\mathbf{u})_{(n-\frac{1}{2},j+1)}], \end{aligned} \quad (5.31)$$

where  $i = 1, 2, \dots, n$  and  $j = 0, 1, \dots, m-1$ .

#### 5.7.4. Gradient on the Y-Component

The discrete gradient on the y- component in 2-D is determined with the scheme as described in [1], [2], and [3].

At the bottom boundary,

$$\begin{aligned} (\text{Gu})_{(i+\frac{1}{2},0)} &= (\text{K}_{22})_{(i+\frac{1}{2},0)} (\tilde{\text{Gu}})_{(i+\frac{1}{2},0)} \\ &+ \left(\frac{1}{2}\right)[(\text{K}_{21})_{(i,\frac{1}{2})} (\tilde{\text{Gu}})_{(i,\frac{1}{2})} + (\text{K}_{21})_{(i+1,\frac{1}{2})} (\tilde{\text{Gu}})_{(i+1,\frac{1}{2})}] \end{aligned} \quad (5.32)$$

On the interior,

$$\begin{aligned} (\text{Gu})_{(i+\frac{1}{2},j)} &= (\text{K}_{22})_{(i+\frac{1}{2},j)} (\tilde{\text{Gu}})_{(i+\frac{1}{2},j)} \\ &+ \left(\frac{1}{4}\right)[(\text{K}_{21})_{(i,j-\frac{1}{2})} (\tilde{\text{Gu}})_{(i,j-\frac{1}{2})} + (\text{K}_{21})_{(i+1,j-\frac{1}{2})} (\tilde{\text{Gu}})_{(i+1,j-\frac{1}{2})} \\ &+ (\text{K}_{21})_{(i,j+\frac{1}{2})} (\tilde{\text{Gu}})_{(i,j+\frac{1}{2})} + (\text{K}_{21})_{(i+1,j+\frac{1}{2})} (\tilde{\text{Gu}})_{(i+1,j+\frac{1}{2})}] \end{aligned} \quad (5.33)$$

At the top boundary,

$$\begin{aligned} (\text{Gu})_{(i+\frac{1}{2},m)} &= (\text{K}_{22})_{(i+\frac{1}{2},m)} (\tilde{\text{Gu}})_{(i+\frac{1}{2},m)} \\ &+ \left(\frac{1}{2}\right)[(\text{K}_{21})_{(i,m-\frac{1}{2})} (\tilde{\text{Gu}})_{(i,m-\frac{1}{2})} + (\text{K}_{21})_{(i+1,m-\frac{1}{2})} (\tilde{\text{Gu}})_{(i+1,m-\frac{1}{2})}] \end{aligned} \quad (5.34)$$

where  $j = 1, 2, \dots, m$  and  $i = 0, 1, \dots, n-1$ .

### 5.8. Tensor Coefficients and the Harmonic Average

As shown in the 2-D Gradient expressions, equations (5.29-5.34), the tensor coefficients are evaluated in the middle of edges for both the x- and y-component. However, according to the definition of tensor coefficients, they are only defined at the centers of the grid cells. Therefore, the tensor coefficients in the middle of edges can be computed by interpolation. The interpolation is performed by using harmonic averages, as it is described by the following:

#### 5.8.1. Tensor Coefficients on the X-Component

At the left boundary,

$$(\text{K}_{uv})_{(0,j+\frac{1}{2})} = (\text{K}_{uv})_{(\frac{1}{2},j+\frac{1}{2})}, \quad (5.35)$$

where  $u, v = 1, 2$  and  $j = 0, 1, \dots, m-1$ .

On the interior,

$$(\text{K}_{uv})_{(i,j+\frac{1}{2})} = \frac{2(\text{K}_{uv})_{(i-\frac{1}{2},j+\frac{1}{2})} (\text{K}_{uv})_{(i+\frac{1}{2},j+\frac{1}{2})}}{(\text{K}_{uv})_{(i-\frac{1}{2},j+\frac{1}{2})} + (\text{K}_{uv})_{(i+\frac{1}{2},j+\frac{1}{2})}}, \quad (5.36)$$

where  $u, v = 1, 2$ ;  $i = 1, 2, \dots, n$ ; and  $j = 0, 1, \dots, m-1$ .

At the right boundary,

$$(\text{K}_{uv})_{(n,j+\frac{1}{2})} = (\text{K}_{uv})_{(n-\frac{1}{2},j+\frac{1}{2})} \quad (5.37)$$

where  $u, v = 1, 2$  and  $j = 0, 1, \dots, m-1$ .

#### 5.8.2. Tensor Coefficients on the Y-Component

At the bottom boundary,

$$(\mathbf{K}_{uv})_{(i+\frac{1}{2},0)} = (\mathbf{K}_{uv})_{(i+\frac{1}{2},\frac{1}{2})}, \quad (5.38)$$

where  $u, v = 1, 2$  and  $i = 0, 1, \dots, m-1$ .

On the interior,

$$(\mathbf{K}_{uv})_{(i+\frac{1}{2},j)} = \frac{2(\mathbf{K}_{uv})_{(i+\frac{1}{2},j-\frac{1}{2})}(\mathbf{K}_{uv})_{(i+\frac{1}{2},j+\frac{1}{2})}}{(\mathbf{K}_{uv})_{(i+\frac{1}{2},j-\frac{1}{2})} + (\mathbf{K}_{uv})_{(i+\frac{1}{2},j+\frac{1}{2})}}, \quad (5.39)$$

where  $u, v = 1, 2$ ;  $j = 1, 2, \dots, m$ ; and  $i = 0, 1, \dots, n-1$ .

At the top boundary,

$$(\mathbf{K}_{uv})_{(i+\frac{1}{2},m)} = (\mathbf{K}_{uv})_{(i+\frac{1}{2},m-\frac{1}{2})}, \quad (5.40)$$

where  $u, v = 1, 2$  and  $i = 0, 1, \dots, n-1$ .

### 5.9. Mimetic Evaluation of $D(\mathbf{Gu})$

Because the Divergence is defined at the centers of the grid cells, the discretization scheme can be determined by the following:

$$D(\mathbf{Gu})_{(i+\frac{1}{2},j+\frac{1}{2})} = \frac{(\mathbf{Gu})_{(i+1,j+\frac{1}{2})} - (\mathbf{Gu})_{(i,j+\frac{1}{2})}}{x} + \frac{(\mathbf{Gu})_{(i+\frac{1}{2},j+1)} - (\mathbf{Gu})_{(i+\frac{1}{2},j)}}{y}, \quad (5.41)$$

where  $i = 0, 1, \dots, n-1$  and  $j = 0, 1, \dots, m-1$ .

### 5.10. Mimetic Implementation of Boundary Condition

In the general case, if Robin boundary conditions are utilized, then the  $B_1$  Boundary operator is applied for the 2-D Discretization with the re-use of equations (4.2) and (4.3) for x- or y-component.

For the x-component or left and right boundary conditions:

$$u \mp (\mathbf{Gu})_{p,j+\frac{1}{2}} = b_{p,j+\frac{1}{2}}, \quad (5.42)$$

and for the y-component or bottom and top boundary conditions:

$$u \mp (\mathbf{Gu})_{i+\frac{1}{2},q} = b_{i+\frac{1}{2},q}. \quad (5.43)$$

in which  $i = 0, 1, \dots, n-1$ ;  $j = 0, 1, \dots, m-1$ ;  $p = 0, n$ ;  $q = 0, m$ ;  $b$  is the boundary right hand side function;  $u$  is the scalar value to drive the Dirichlet term; and  $\mp$  is the scalar value to drive the Neumann term.

### 5.11. 2-D Mimetic Discrete Equation System

By combining all of the Mimetic Operator expressions, equations (5.23) – (5.43), a linear matrix equation system will be resulted with the size of  $(M \times M)$  with  $M = nm + 2(n + m)$ ,  $n$  be the number of divided sub-intervals in the x-component, and  $m$  be the number of divided sub-intervals in the y-component.

## 6. NUMERICAL ERROR COMPUTATION

The errors and the convergence rates for the Mimetic method are computed using the mean square norm and the maximum norm for various test problems. The mean square norm is defined in [5] take the form in 1-D:

$$E_{L_2} = \|U - p_h u\|_{L_2} = [(U_0 - u(x_0))^2 h_{1/2} + \sum_{i=0}^{n-1} (U_{i+1/2} - u(x_{i+1/2}))^2 h_{i+1/2} + (U_n - u(x_n))^2 h_{n-1/2}]^{1/2}, \quad (6.1)$$

and in 2-D:

$$E_{L_2} = \|U - p_h u\|_{L_2} = \left\{ \sum_{i=0}^{n-1} (U_{i+1/2,0} - u(x_{i+1/2}, y_0))^2 (x_{i+1/2} * y_{1/2}) + \sum_{i=0}^{n-1} (U_{i+1/2,m} - u(x_{i+1/2}, y_m))^2 (x_{i+1/2} * y_{m-1/2}) + \sum_{(i,j)=(0,0)}^{(n-1,m-1)} (U_{i+1/2,j+1/2} - u(x_{i+1/2}, y_{j+1/2}))^2 (x_{i+1/2} * y_{j+1/2}) + \sum_{j=0}^{m-1} (U_{0,j+1/2} - u(x_0, y_{j+1/2}))^2 (x_{1/2} * y_{j+1/2}) + \sum_{j=0}^{m-1} (U_{n,j+1/2} - u(x_n, y_{j+1/2}))^2 (x_{n-1/2} * y_{j+1/2}) \right\}^{1/2}. \quad (6.2)$$

The max norm is obtained by the following:

For 1-D,

$$E_{\max} = \|U - p_h u\|_{\max} = \max \left| \max_{i=0,n} |U_i - u(x_i)|, \max_{i=0}^{n-1} |U_{i+1/2} - u(x_{i+1/2})| \right|, \quad (6.3)$$

and for 2-D,

$$E_{\max} = \|U - p_h u\|_{\max} = \max \left| \max_{i=0}^{n-1} |U_{i+1/2,0} - u(x_{i+1/2}, y_0)|, \max_{i=0}^{n-1} |U_{i+1/2,m} - u(x_{i+1/2}, y_m)|, \max_{(i,j)=(0,0)}^{(n-1,m-1)} |U_{i+1/2,j+1/2} - u(x_{i+1/2}, y_{j+1/2})|, \max_{j=0}^{m-1} |U_{0,j+1/2} - u(x_0, y_{j+1/2})|, \max_{j=0}^{m-1} |U_{n,j+1/2} - u(x_n, y_{j+1/2})| \right|, \quad (6.4)$$

in which  $U_{i+1/2}$  or  $U_{i+1/2, j+1/2}$  represent the approximations given by the scheme to the exact solution  $u(x_{i+1/2})$  or  $u(x_{i+1/2}, y_{j+1/2})$  respectively.

In general, the order of convergence  $q$  can be approximated with:

$$q = \frac{\log(\frac{E_1}{E_2})}{\log(\frac{h_1}{h_2})}, \quad (6.5)$$

where  $h_1$  and  $h_2$  are the grid sizes of the sub-intervals producing the truncation errors,  $E_1$  and  $E_2$  respectively, and it is supposed that  $h_1 > h_2$ ; hence,  $E_1 > E_2$ . If the approximated scheme is in 2-D,  $h_1$  and  $h_2$  above are computed by  $h_1 = \max(x_1, y_1)$  and  $h_2 = \max(x_2, y_2)$ . The convergence rate or the order of the convergences for the max norm errors and the mean square norm errors should be approximately equal to each other. In this case, the approximation should be convergent to second order.

## 7. ONE-DIMENSIONAL TEST CASES

The 1-D schemes on uniform and non-uniform grids were used to solve this particular boundary value problem.

Problem 1:

$$-\frac{d^2u(x)}{dx^2} = f(x) \text{ on } [0,1], \quad (7.1)$$

with the Robin boundary conditions:

$$u(0) - u'(0) = -1, \quad (7.2)$$

$$u(1) + u'(1) = 0, \quad (7.3)$$

where:

$$\begin{aligned} f(x) &= \frac{-e^{-2x}}{e^{-1}-1}, \\ &= -e^{-2x}, \\ &= \frac{e^{-2x}-1}{e^{-1}-1}, \\ &= -1. \end{aligned}$$

### 7.1. 2-2-2 Scheme on 1-D Uniform Grids

As depicted in tables 7.1 and 7.2, both the mean square errors and the max errors showed second order convergence, which was compliant with the analysis of the second order Mimetic Operators. Moreover, the solutions of the discretization, which includes the  $\tilde{B}$  boundary operator, had slightly smaller errors than those using the  $B$  boundary operator when uniform grids were used.

**Table 7.1. Results for 2-2-2 Scheme on Uniform Grids with  $B_1$  Operator**

| n   | Mean Square |        | Max      |        |
|-----|-------------|--------|----------|--------|
|     | Error       | Order  | Error    | Order  |
| 100 | 3.36E-06    |        | 6.23E-06 |        |
| 200 | 8.31E-07    | 2.0167 | 1.56E-06 | 1.9998 |
| 400 | 2.07E-07    | 2.0087 | 3.92E-07 | 2.0000 |

**Table 7.2. Results for 2-2-2 Scheme on Uniform Grids with  $\tilde{\mathbf{B}}$  Operator**

| n   | Mean Square |        | Max      |        |
|-----|-------------|--------|----------|--------|
|     | Error       | Order  | Error    | Order  |
| 100 | 3.29E-06    |        | 6.28E-06 |        |
| 200 | 8.21E-07    | 2.0011 | 1.57E-06 | 1.9998 |
| 400 | 2.05E-07    | 2.0004 | 3.92E-07 | 2.0000 |

A deep analysis and investigation of the comparison in errors between  $\tilde{\mathbf{B}}$  and  $\mathbf{B}_1$  Operators could also be found in [7].

## 7.2. 2-2-2 Scheme on 1-D Non-Uniform Grids

In generating non-uniform grids with n different grid sizes, a smooth function was utilized over the interval [a, b] with each node having a coordinate at [10]:

$$x_i = \left[ a + \frac{b-a}{n} (i) \right]^2, \quad (7.4)$$

where,  $i = 0, \dots, n$ ;  $x_0 = a$ ; and  $x_n = b$  since  $a = 0$  and  $b = 1$ .

Similarly, as shown in tables 7.3 and 7.4, both the mean square errors and the max errors were convergent to the second order approximation by using the 2-2-2 Mimetic discretization scheme on non-uniform grids. The discretization with the  $\tilde{\mathbf{B}}$  Operator presents better results in terms of errors induced than those with the  $\mathbf{B}_1$  Operators.

**Table 7.3. Results for 2-2-2 Scheme on Non-Uniform Grids with  $\mathbf{B}_1$  Operator**

| n  | Mean Square |        | Max      |        |
|----|-------------|--------|----------|--------|
|    | Error       | Order  | Error    | Order  |
| 10 | 2.40E-03    |        | 3.60E-03 |        |
| 20 | 5.41E-04    | 2.1505 | 9.01E-04 | 1.9980 |
| 40 | 1.26E-07    | 2.1022 | 2.25E-04 | 2.0026 |

**Table 7.4. Results for 2-2-2 Scheme on Non-Uniform Grids with  $\tilde{\mathbf{B}}$  Operator**

| n  | Mean Square |        | Max      |        |
|----|-------------|--------|----------|--------|
|    | Error       | Order  | Error    | Order  |
| 10 | 2.20E-03    |        | 3.40E-03 |        |
| 20 | 5.20E-04    | 2.0808 | 8.79E-04 | 1.9517 |
| 40 | 1.24E-07    | 2.0709 | 2.22E-04 | 1.9855 |

## 8. TWO-DIMENSIONAL TEST CASES ON UNIFORM GRIDS

The elliptic PDE given in equation (5.2) was written as,

$$-\operatorname{div}(\mathbf{K} \operatorname{grad} u) = f(x, y), \quad (8.1a)$$

using the discrete operators, equation (8.1a) becomes

$$-\mathbf{D}(\mathbf{K} \mathbf{G}u) = f(x, y) \quad (8.1b)$$

With the exception of Problem 2 which is explained below, if Robin boundary conditions are applied, then equations (5.42) and (5.43) are used with  $\alpha$  and  $\beta$  both set to 1. On the other hand, if Dirichlet Boundary Conditions are applied, then equations (5.42) and (5.43) are used with  $\alpha$  equal to 1 and  $\beta$  set to 0.

### 8.1. Discretization with Identity Tensor

Problem 2: the 2-D differential equation (8.1b) defined on  $[0, 1] \times [0, 1]$  includes the right hand side equation,  $f(x, y)$  which is set to:

$$f(x, y) = \frac{e^{\frac{(x+y)}{2}}}{2 * (e - 1)}, \text{ for } \alpha = 1. \quad (8.2)$$

The  $\alpha$  and  $\beta$  values from Robin Boundary Conditions of equations (5.42) and (5.43) are set as

$$\alpha = -e, \quad (8.3)$$

$$\beta = \frac{e - 1}{2}. \quad (8.4)$$

The Identity tensor is defined with

$$K = \begin{bmatrix} 1 & 0 \\ 0 & 1 \end{bmatrix} \quad (8.5)$$

Tensor K corresponds to identity tensor introduced in equation (8.1a). Thus, the exact solution for this problem is given with

$$u_{\text{exact}}(x, y) = \frac{e^{\frac{(x+y)}{2}}}{(e - 1)}. \quad (8.6)$$

The application of Mimetic discretization was obviously straightforward since the tensor was an identity matrix. Both the mean square errors and the max errors, as obtained in table 8.1, were shown to be convergent on the second order approximation.

**Table 8.1. Results for Problem 2 Using Robin Boundary Conditions**

| n  | Mean Square |        | Max      |        |
|----|-------------|--------|----------|--------|
|    | Error       | Order  | Error    | Order  |
| 10 | 4.56E-05    |        | 1.04E-04 |        |
| 20 | 1.08E-05    | 2.0792 | 2.86E-05 | 1.8645 |
| 40 | 2.57E-06    | 2.0699 | 7.49E-06 | 1.9331 |

### 8.2. Discretization with Diagonal Tensor

The following problem was solved in [3] by the C-square Grid Method.

Problem 3: the right hand side function of the (PDE) equation (8.1b) is defined on  $[0, 1] \times [0, 1]$ ,

$$f(x, y) = -[60xy + 12y^2 - 11\sin(x)\cos(y)]. \quad (8.7)$$

Both Dirichlet and Robin Boundary Conditions are investigated and the diagonal tensor matrix is as follows:

$$K = \begin{bmatrix} 10 & 0 \\ 0 & 1 \end{bmatrix}. \quad (8.8)$$

Thus, the exact solution to the PDE defined on  $[0, 1] \times [0, 1]$  is,

$$u = x^3 y + y^4 + \sin(x) \cos(y). \quad (8.9)$$

Results from using the Mimetic method in the case of Dirichlet Boundary Conditions were determined and displayed in table 8.2, which also includes the results of C-square Grids from [3] as a comparison.

The diagonal tensor with  $K_{11} (= 10)$  is much larger than  $K_{22} (= 1)$ , i.e., the tensor coefficient for the gradient in the x-component was larger than the tensor coefficient for the gradient in the y-component. The attempt was to create unbalanced gradient terms between the x- and y-component in the discretization. As a result, the equation system becomes much more unstable and difficult to solve in comparison to the identity tensor approach. For both Dirichlet and Robin Boundary Conditions, the mean square errors and the max errors were convergent to the second order approximation, as shown in tables 8.2 and 8.3. In addition, the Mimetic method introduced considerably smaller errors than C-Square Grid Method from [3] with the same degree of complexity or number of divided grids as applied to the Dirichlet Boundary Conditions, shown in table 8.2.

**Table 8.2. Results for Problem 3 Using Dirichlet Boundary Conditions**

| n  | Mean Square     |                        |                 | Max             |                 |
|----|-----------------|------------------------|-----------------|-----------------|-----------------|
|    | Error (Mimetic) | Error (C-Square Grids) | Order (Mimetic) | Error (Mimetic) | Order (Mimetic) |
| 10 | 2.90E-04        | 3.73E-04               |                 | 9.09E-04        |                 |
| 17 | 7.53E-05        | 1.21E-04               | 2.5387          | 2.26E-04        | 2.6237          |
| 20 | 5.09E-05        | 8.54E-05               | 2.4074          | 1.44E-04        | 2.7658          |
| 33 | 1.65E-05        | 2.95E-05               | 2.2456          | 3.48E-05        | 2.8384          |
| 65 | 4.11E-06        | 6.96E-06               | 2.0542          | 6.87E-06        | 2.3931          |

**Table 8.3. Results for Problem 3 Using Robin Boundary Conditions**

| n  | Mean Square |        | Max      |        |
|----|-------------|--------|----------|--------|
|    | Error       | Order  | Error    | Order  |
| 10 | 4.00E-03    |        | 4.40E-03 |        |
| 17 | 1.30E-03    | 2.1181 | 1.50E-03 | 2.0280 |
| 20 | 9.67E-04    | 1.8182 | 1.10E-03 | 1.9084 |
| 33 | 3.51E-04    | 2.0261 | 4.17E-04 | 1.9387 |
| 65 | 8.95E-05    | 2.0151 | 1.08E-04 | 1.9867 |

### 8.3. Discretization with Full Tensor

The following problem was solved by the Support Operator Method and results could be found [9].

Problem 4: the right hand function for the elliptic PDE equation (8.1) is defined on  $[0, 1] \times [0, 1]$  by the following:

$$f(x, y) = -2(1 + x^2 + xy + y^2)e^{xy}. \quad (8.10)$$

The tensor  $K$  corresponds to the full matrix:

$$K = \begin{bmatrix} 2 & 1 \\ 1 & 2 \end{bmatrix}. \quad (8.11)$$

Therefore, the exact solution to this problem is given by:

$$u = e^{xy}. \quad (8.12)$$

In case of Dirichlet Boundary Conditions, results are determined by the Mimetic Numerical Method and compared against the ones obtained by the Support Operator method [9], shown as in table 8.4.

**Table 8.4. Results for Problem 4 Using Dirichlet Boundary Conditions**

| n  | Mean Square     |                        |                 | Max             |                 |
|----|-----------------|------------------------|-----------------|-----------------|-----------------|
|    | Error (Mimetic) | Error (Supp. Operator) | Order (Mimetic) | Error (Mimetic) | Order (Mimetic) |
| 10 | 1.80E-03        |                        |                 | 4.40E-03        |                 |
| 17 | 6.21E-04        | 1.06E-03               | 2.0067          | 1.60E-03        | 1.9064          |
| 20 | 4.49E-04        |                        | 1.9872          | 1.20E-03        | 1.7701          |
| 33 | 1.66E-04        | 2.58E-04               | 1.9907          | 4.48E-04        | 1.9660          |
| 65 | 4.29E-05        | 6.36E-05               | 1.9945          | 1.18E-04        | 1.9691          |

As the tensor was extended to a full matrix from a diagonal one, the complexity of the discretization increased dramatically. However, the element values of the tensor were relatively small ranging from 1 to 2. Hence, although the left-hand side matrix of the equation system resulting from the discretization was far more populated when going from a diagonal tensor to a full tensor, the equation system from the full tensor was much more stable when comparing its condition numbers to those of the diagonal tensor case. As shown in tables 8.4 and 8.5 for both Dirichlet and the Robin Boundary Conditions respectively. The mean square errors and the max errors were consistently convergent to second order of approximation. The Mimetic method had far better results than the Support Operator Method when applying Dirichlet Boundary Condition. Especially at  $n = 17, 33,$  and  $65,$  the Mimetic method introduced substantially smaller errors than the Support Operator Method.

**Table 8.5. Results for Problem 4 Using Robin Boundary Conditions**

| n  | Mean Square |        | Max      |        |
|----|-------------|--------|----------|--------|
|    | Error       | Order  | Error    | Order  |
| 10 | 2.20E-03    |        | 8.00E-03 |        |
| 17 | 7.58E-04    | 2.0088 | 3.50E-03 | 1.5579 |
| 20 | 5.44E-04    | 2.0408 | 2.60E-03 | 1.8290 |
| 33 | 1.96E-04    | 2.0374 | 1.10E-03 | 1.7177 |
| 65 | 4.96E-05    | 2.0277 | 3.54E-04 | 1.6725 |

### 8.4. Discretization with Full and Discontinuous Tensor

The following problem was solved by the Support Operator method in [9].

Problem 5: the right-hand side function to the elliptic PDE equation (8.1) as defined on  $[-1, 1] \times [-1, 1]$  with a discontinuity at  $x = 0$  is defined as

$$f(x, y) = \begin{cases} (2\sin y + \cos y)\varphi x + \sin y & \text{if } x < 0 \\ -2\varphi \exp(x)\cos(y) & \text{if } x > 0. \end{cases} \quad (8.13)$$

The full tensor matrix,  $K$ , with the continuity at  $x = 0$ , is

$$K = \begin{cases} \begin{bmatrix} 1 & 0 \\ 0 & 1 \end{bmatrix} & \text{if } x < 0 \\ \varphi \begin{bmatrix} 2 & 1 \\ 1 & 2 \end{bmatrix} & \text{if } x > 0. \end{cases} \quad (8.14)$$

And the exact solution to the PDE is

$$u = \begin{cases} (2\sin y + \cos y)\varphi x + \sin y & \text{if } x < 0 \\ e^x \sin(y) & \text{if } x > 0, \end{cases} \quad (8.15)$$

in which  $\varphi = 1$ .

Because of this discontinuity, results are obtained as the combination of two defined two-unit rectangles,  $([-1, 0] \times [-1, 1])$  and  $([0, 1] \times [-1, 1])$  which are  $(x < 0)$  and  $(x > 0)$  zones, respectively.

The Mimetic Method results for the Dirichlet Boundary Conditions were computed and the results for the Support Operator Method from [9] are shown in table 8.6. In addition, the Mimetic results for the Robin Boundary Conditions are shown in table 8.7.

**Table 8.6. Results for Problem 5 Using Dirichlet Boundary Conditions**

| n  | Mean Square     |                        |                 | Max             |                 |
|----|-----------------|------------------------|-----------------|-----------------|-----------------|
|    | Error (Mimetic) | Error (Supp. Operator) | Order (Mimetic) | Error (Mimetic) | Order (Mimetic) |
| 14 | 4.20E-03        |                        |                 | 4.90E-03        |                 |
| 16 | 3.20E-03        | 7.05E-03               | 2.0365          | 3.80E-03        | 1.9039          |
| 20 | 2.00E-03        |                        | 2.1063          | 2.40E-03        | 2.0594          |
| 32 | 7.94E-04        | 1.73E-03               | 1.9661          | 9.68E-04        | 1.9314          |
| 64 | 1.98E-04        | 3.96E-04               | 2.0028          | 2.45E-04        | 1.9801          |

**Table 8.7. Results for Problem 5 Using Robin Boundary Conditions**

| n  | Mean Square |        | Max      |        |
|----|-------------|--------|----------|--------|
|    | Error       | Order  | Error    | Order  |
| 14 | 5.30E-03    |        | 5.90E-03 |        |
| 17 | 4.00E-03    | 2.1075 | 4.70E-03 | 1.7029 |
| 20 | 2.50E-03    | 2.1063 | 3.40E-03 | 1.4510 |
| 33 | 9.75E-04    | 2.0041 | 1.60E-03 | 1.6038 |
| 65 | 2.39E-04    | 2.0275 | 5.30E-04 | 1.5948 |

If  $x < 0$ , then the tensor was the identity matrix, whereas in case of  $x > 0$ , the tensor was a full matrix, but with relatively small coefficients. The two sets of results were then combined to determine the errors. According to the results from tables 8.6 and 8.7, both the mean square errors and the max errors were convergent to second order approximation. Importantly, the Mimetic method improved the mean square errors by approximately a half as compared to the Support Operator Method for Dirichlet Boundary Conditions.

### 8.5. Discretization with Full Tensor as a Relatively Hard Example

This problem was solved by the Uniform Cell Centered method and results could be found in [3].

Problem 6: The right-hand side function to the elliptic PDE equation (8.1) defined on  $[0, 1] \times [0, 1]$  is given as

$$f(x, y) = -[-22(y - y^2) - 26(x - x^2) + 18(1 - 2x)(1 - 2y)], \quad (8.16)$$

where, the full tensor matrix with large coefficients is

$$K = \begin{bmatrix} 11 & 9 \\ 9 & 13 \end{bmatrix}. \quad (8.17)$$

The exact solution to the problem is given by

$$u = (x - x^2)(y - y^2). \quad (8.18)$$

In the case of Dirichlet Boundary Conditions, results obtained by the Mimetic method were computed and displayed, as well as the ones from the Uniform Cell Centered method in tables 8.8 and 8.9.

**Table 8.8. Results for Problem 6 Using Dirichlet Boundary Conditions**

| n  | Mean Square     |                       |                 | Max             |                 |
|----|-----------------|-----------------------|-----------------|-----------------|-----------------|
|    | Error (Mimetic) | Error (Cell-Centered) | Order (Mimetic) | Error (Mimetic) | Order (Mimetic) |
| 10 | 5.73E-04        | 2.34E-02              |                 | 1.20E-03        |                 |
| 17 | 2.08E-04        | 8.09E-03              | 1.9136          | 4.43E-04        | 1.8768          |
| 20 | 1.51E-04        | 5.85E-03              | 1.9428          | 3.25E-04        | 1.9081          |
| 33 | 5.67E-05        | 2.15E-03              | 1.9603          | 1.23E-04        | 1.9351          |
| 65 | 1.48E-05        | 5.54E-04              | 1.9792          | 3.31E-05        | 1.9415          |

**Table 8.9. Results for Problem 6 Using Robin Boundary Conditions**

| n  | Mean Square |        | Max      |        |
|----|-------------|--------|----------|--------|
|    | Error       | Order  | Error    | Order  |
| 10 | 1.50E-03    |        | 4.80E-03 |        |
| 17 | 5.27E-04    | 1.9699 | 2.50E-03 | 1.2293 |
| 20 | 3.80E-04    | 2.0173 | 2.00E-03 | 1.3730 |
| 33 | 1.36E-04    | 2.0565 | 9.72E-04 | 1.4406 |
| 65 | 3.31E-05    | 2.0801 | 3.38E-04 | 1.5586 |

The full tensor coefficients were relatively large ranging from 9 to 13 (i.e. much greater than 1), but the diagonal tensor values were close to each other. Consequently, the x- and y-component of the gradient become balanced. However, because of these values of tensor coefficients, the problem was considered to be a relatively hard example. For both Dirichlet and Robin Boundary Conditions, the mean square errors and the max errors were convergent to second order approximation, as shown in tables 8.8 and 8.9 respectively. More importantly, the Mimetic method had improved the errors up to the order of  $10^{-2}$  in comparison to the Uniform Cell-Centered method, in case of Dirichlet Boundary Conditions.

## 9. CONCLUSION

The second order Mimetic discretization method has been used to solve a general elliptic partial equation in 1-D and 2-D space. The method was applied on 1-D staggered grids and 2-D staggered rectangular or square grids. All of the results were consistent to obtain the second order approximation as expected. The essential advantage of this method over others was the capability of the Mimetic Operators to obtain a second order approximation at the boundary as well as in the interior grids. Hence, its overall performance yielded smaller mean square errors when compared to similar methodologies.

In 1-D, both cases of uniform and non-uniform grids gave second order approximation for mean square errors and max errors. In addition, the  $\tilde{B}$  boundary operator, which results from the discrete Divergence and Gradient operators satisfying a discrete analogue of the divergence theorem, provided slightly better results than those from the simple  $B_1$  boundary operator.

In 2-D, the discretizations became more complicated after incorporating matrix tensor coefficients in comparison to the 1-D case, although it was implemented on uniform grids. The tested numerical examples varied from diagonal to full, from continuous to discontinuous, and from small to big values for the tensor coefficients. Results obtained were convergent to the second order approximation in both measured mean square and max errors. Specially, the Mimetic method had shown a substantial improvement over other methods in terms of minimizing mean square errors.

As for any future work, the following tasks should be considered:

1. Second order operators should be investigated on non-orthogonal meshes instead of a uniform square or on rectangular grids in 2-D.
2. High order Mimetic Operators, such as fourth or sixth order discrete operators should be employed on square, rectangular, or non-orthogonal grids such as tetrahedral grids.
3. On a 3-D mesh, the problem for discretization could become very complex. A concrete scheme for this particular investigation should be wisely constructed using high order Mimetic operators and thoroughly developed minimizing the complexity that discretization on 3-D grid volumes might create.

## ACKNOWLEDGEMENTS

We would like to thank Otilio Rojas for his helpful suggestions to improve the paper. We also would like to thank NSF and DOE for the support on the PASI.

## REFERENCES

1. T. Arbogast, P. T. Keenan, M. F. Wheeler, and I. Yotov (1995), Logically Rectangular Mixed Methods For Darcy Flow On General Geometry, SPE 29099, in Proceedings of the 13th SPE Symposium on Reservoir Simulation, *Society of Petroleum Engineers*, Richardson, Texas, pp. 51-59.
2. T. Arbogast, M. F. Wheeler, and I. Yotov (1994), Logically Rectangular Mixed Methods For Groundwater Flow and Transport on General Geometry, *Computational Methods in Water Resources X*, Vol. 1, A. Peters, G. Whittum, B. Herrling, U. Meissner, C. A. Brebbia, W. G. Gray, and G. F. Pindar, eds., *Kluwer Academic Publishers*, Dordrecht, The Netherlands, pp. 149-156.
3. T. Arbogast, M. F. Wheeler, and Ivan Yotov (1997), Mixed Finite Elements for Elliptic Problems with Tensor Coefficients as Cell-Centered Finite Differences, *SIAM Numer. Anal.*, 34, pp. 828-852.
4. J. E. Castillo and R. Grone (2003), A Matrix Analysis Approach to Higher-Order Approximations for Divergence and Gradients Satisfying a Global Conservation Law, *SIAM J. Matrix Anal. Appl.*, 25.
5. J. E. Castillo, J. M. Hyman, M. J. Shashkov, S. Steinberg (1996), High Order Mimetic Finite Difference Methods on Nonuniform Grids, *Proceedings of the Third International Conference on Spectral and High Order methods*, Houston.
6. J. E. Castillo and M. Yasuda (2003), A comparison of Two Matrix Operator Formulations for Mimetic Divergence and Gradient Discretizations, *Proceedings of the International Conference on Parallel and Distributed Processing Techniques and Applications*, Volume III.
7. J.E. Castillo, and M. Yasuda (2005), Linear Systems Arising for Second-Order Mimetic Divergence and Gradient Discretizations, *Journal of Mathematical Modeling and Algorithms*, 4, pp. 67-82.
8. B. Das, T. H. Robey, S. Steinberg, and D. Zang (1994), Comparisons of numerical solution methods for differential equations with discontinuous coefficients, *Mathematics and Computers in Simulation* 36, 57.
9. J. Hyman, M. Shashkov, and S. Steinberg (1997), The Numerical Solution of Diffusion Problems in Strongly Heterogeneous Non-Isotropic Materials, *Journal of Computational Physics* 132, pp. 130-148.
10. S. Rojas, J. Castillo, J. Guevara, and S. Castillo (2004), A Comparative Numerical Study of two Mimetic Finite Difference Methods for Solving the Steady Diffusion Equation with Rough Coefficients on Non-uniform Grids, *Simulación Numérica y Modelaje Computacional*, edited by J. Rojo, M. J. Torres, and M. Cerrolaza, pp. TM1.